Organic & Biomolecular Chemistry

PAPER

View Article Online
View Journal | View Issue

Cite this: *Org. Biomol. Chem.*, 2014, **12**, 8911

The design, synthesis and biological evaluation of novel thiamin diphosphate analog inhibitors against the pyruvate dehydrogenase multienzyme complex E1 from *Escherichia coli*†

Lingling Feng,[a] Junbo He,[a,b] Haifeng He,[a] Lulu Zhao,[a] Lingfu Deng,[c] Li Zhang,[a] Lin Zhang,[a] Yanliang Ren,[a] Jian Wan*[a] and Hongwu He*[a]

Received 28th June 2014,
Accepted 18th September 2014

DOI: 10.1039/c4ob01347f

www.rsc.org/obc

Pyruvate dehydrogenase multienzyme complex E1 (PDHc E1) is a potential target enzyme when looking for inhibitors to combat microbial disease. In this study, we designed and synthesized a series of novel thiamin diphosphate (ThDP) analogs with triazole ring and oxime ether moieties as potential inhibitors of PDHc E1. Their inhibitory activities against PDHc E1 were examined both *in vitro* and *in vivo*. Most of the tested compounds exhibited moderate inhibitory activities against PDHc E1 (IC_{50} = 6.1–75.5 μM). The potent inhibitors **4g**, **4h** and **4j**, had strong inhibitory activities with IC_{50} values of 6.7, 6.9 and 6.1 μM against PDHc E1 *in vitro* and with inhibition rates of 35%, 50% and 33% at 100 μg mL^{-1} against *Gibberella zeae in vivo*, respectively. The binding mode of **4j** to PDHc E1 was analyzed by a molecular docking method. Furthermore, the possible interactions of the important residues of PDHc E1 with compound **4j** were examined by site-directed mutagenesis, enzymatic assays and spectral fluorescence studies. The theoretical and experimental results are in good agreement and suggest that compound **4j** could be used as a lead compound for further optimization, and may have potential as a new microbicide.

1. Introduction

Pathogenic microbes such as *Botrytis cinerea*, *Gibberella zeae*, *Rhizoctonia solani*, and *Escherichia coli* are hazardous to modern agriculture and human health.[1,2] Although there are microbicides (carbendazim, pyrimethanil, and ciprofloxacin) that can be used for these pathogenic microbial infections, the severe side effects and toxicity of these microbicides and the increasing resistance to these microbicides have been recorded worldwide and are important factors resulting in treatment failure.[3,4] Therefore, it is of general interest to develop a new and efficient microbicide with novel structures or modes of action, or even new drug targets to help overcome microbial disease.

The pyruvate dehydrogenase multienzyme complex (PDHc) plays a vital role in cellular metabolism and catalyzes the oxidative decarboxylation of pyruvate, and the subsequent acetylation of coenzyme A (CoA) to acetyl-CoA, during the tricarboxylic acid metabolic pathway.[5] PDHc contains three enzymatic components: pyruvate dehydrogenase (E1), dihydrolipoamide acetyltransferase (E2), and dihydrolipoamide dehydrogenase (E3).[5] The pyruvate dehydrogenase (PDHc E1) portion has two active sites: the substrate binding site and the cofactor thiamin diphosphate (ThDP) binding site. PDHc E1 catalyzes the first step of this complex process and is an important target enzyme when finding inhibitors.[6]

Much effort has been made to design and synthesize inhibitors of PDHc E1 including the PDHc E1 substrate analogs and cofactor ThDP analogs (Fig. 1).[7–12] These ThDP analog inhibitors, such as thiamin thiazolone diphosphate (ThTDP) and thiamine thiothiazolone diphosphate (ThTTDP), can block the formation of a covalent adduct between the substrate pyruvate and cofactor ThDP through the C2 atom of the thiazolium ring in the reaction pathway for PDHc E1.[11–15] These ThDP analog inhibitors exhibit significantly stronger binding affinities for PDHc E1 than ThDP and have received increasing attention.[13] However, due to their complex structure with highly charged pyrophosphate groups, these ThDP analogs exhibit no potential utility and display poor bioavailability.[11–15]

The crystal structures of the PDHc E1/ThDP complex and the PDHc E1/inhibitor (ThTDP) complex from *E. coli* (PDB ID: 1L8A and 1RP7) have been determined.[14,15] These structures

[a]*Key Laboratory of Pesticide & Chemical Biology (CCNU), Ministry of Education, College of Chemistry, Central China Normal University, Wuhan 430079, China. E-mail: jianwan@mail.ccnu.edu.cn, he1208@mail.ccnu.edu.cn; Fax: +86-27-67862022, +86-27-67867960; Tel: +86-27-67862022, +86-27-67867960*
[b]*College of Food Science and Engineering, Wuhan Polytechnic University, Wuhan 430023, China*
[c]*College of Life Science, Central China Normal University, Wuhan 430079, China*
† Electronic supplementary information (ESI) available. See DOI: 10.1039/c4ob01347f

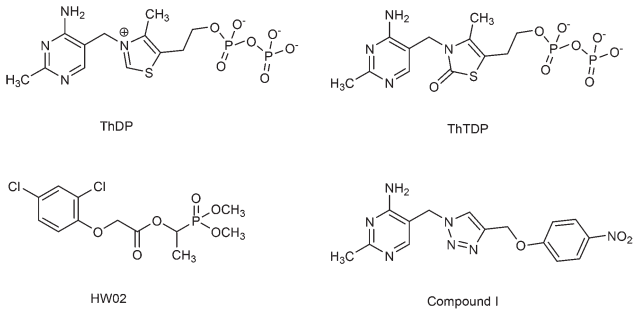

Fig. 1 Structures of ThDP and the known potential ThDP analog inhibitors of PDHc E1.

reveal detailed characterization of the active site of PDHc E1, and provide a solid basis for understanding the structure and mechanism. They enable structure-based design of novel inhibitors against PDHc E1. In our laboratory, we carried out a systematic study for the design and synthesis of inhibitors against PDHc E1 as a herbicide (HW02) (Fig. 1).[16] The mechanism was predicted with theory.[17,18] The herbicide HW02 was found to be an effective inhibitor against PDHc E1. Docking studies were employed to shed light on the binding mode of the interactions.

The triazole ring moiety can be tuned to form powerful pharmacophores and plays an important role in bio-conjugation. Furthermore, it is a useful building block in organic synthesis because of its wide range of biological activities.[19,20] The oxime ether derivatives have attracted recent attention in medicinal chemistry research due to their excellent antibacterial, antifungal or antimicrobial activities.[21–24] These results encouraged us to explore and design novel ThDP analog inhibitors against PDHc E1 that possess microbicide activity by introducing the triazole ring and oxime ether moieties. Here we report the design and synthesis of a series of new compounds incorporating the active triazole ring and oxime ether pharmacophores and evaluate their inhibitory activities against PDHc E1 from *E. coli*. Furthermore, the mode of interaction of the important residues of PDHc E1 with the hit compound was examined by molecular docking experiments, site-directed mutagenesis, and enzymatic assays.

2. Results and discussion

2.1 Design and synthesis of new ThDP analog inhibitors (4a–4l)

The crystal structures of the PDHc E1/ThDP complex and the PDHc E1/inhibitor (ThTDP) complex from *E. coli* (PDB ID: 1L8A and 1RP7) provides detailed characterization of the active site of PDHc E1 and facilitates our design of new ThDP inhibitors targeted to the active site of PDHc E1.[14,15] The ThDP consists of three parts: diphosphate group, aminopyrimidine, and thiazolium moiety, which are bound in a "V" conformation involving the N-terminal and middle domains of PDHc E1.[14] Due to the excellent antibacterial, antifungal, and antimicrobial activities of the oxime ether as well as the high charge of the pyrophosphate group, we expect that the oxime ether moiety of the new inhibitor (shown in red) can substitute for the diphosphate group and avoid the high charge of the pyrophosphate group (Fig. 2).[13,21–24]

PDHc E1 is initiated by the formation of a covalent adduct between the substrate and the cofactor through the C2 atom of the thiazolium ring in the reaction pathway of PDHc E1.[14,15] The triazole ring moiety has a surprisingly stable structure with three adjacent nitrogen atoms, has a wide range of biological activities, and also plays an important role in bio-conjugation.[19,20] We expected that the new inhibitor with the triazole ring moieties would block this site by replacing the proton on C2 with a nitrogen atom in the triazole ring moieties (shown in blue) of the novel ThDP analog inhibitors (Fig. 2). The aminopyrimidine ring was maintained for the proper orientation of the newly designed inhibitors because the aminopyrimidine ring hydrogen bonds to the active site of PDHc E1, which is partly responsible for the proper orientation of the cofactor ThDP.[14] The structure of the new inhibitor is shown as Fig. 2.

The synthetic route used for compounds **4a–4l** is depicted in Scheme 1. Intermediates **1a–1l** were synthesized using various substituted benzaldehydes or acetophenones and react with hydroxylamine hydrochloride in the presence of potassium carbonate.[25] Compounds **1a–1l** were then converted into intermediates **2a–2l** in the presence of 3-bromopropyne using NaOH as the base.[26] The 5-azidomethyl-2-methylpyrimidine-4-ylamine **3** was readily prepared from thiamine hydrochloride (ThDP) according to a literature report.[27] Finally, the Cu-catalyzed 1,3-dipolar cycloaddition reaction was used to assemble the oxime ether **4a–4l** employing copper(I) iodide-triethylamine (TEA) in THF.[28] The oxime-ether compounds are stable in the solid and solution states. The final compounds **4a–4l** were purified by recrystallization from dimethyl formamide-water and characterized by ^{1}H NMR, ^{13}C NMR, mass spectrometry (MS), and elemental analysis.

2.2 Inhibitory activities of the new ThDP analog inhibitors (4a–4l) against *E. coli* PDHc E1

The synthesized ThDP analog inhibitors (**4a–4l**) were evaluated for their inhibitory activities (half maximal inhibitory

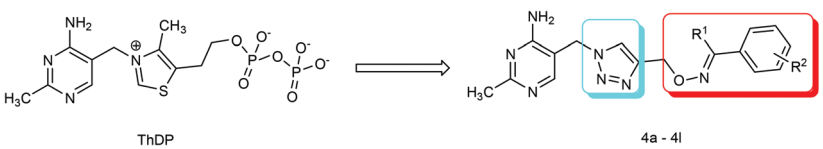

Fig. 2 Design of novel thiamin diphosphate (ThDP) inhibitors of PDHc E1.

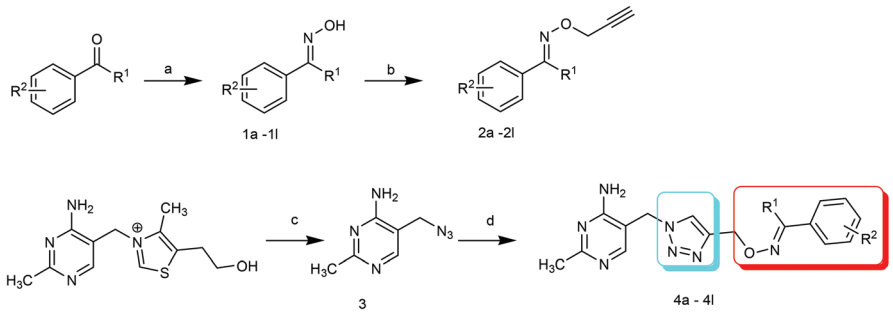

Scheme 1 Synthetic pathway of novel thiamin diphosphate (ThDP) **4a–4l**. Reagents and conditions: (a) $NH_2OH{\cdot}HCl$, K_2CO_3, EtOH, reflux, 7 h; (b) 3-Bromopropyne, NaOH, CH_3CN, reflux, 8 h; (c) NaN_3, $Na_2S_2O_3$, H_2O, 60–65 °C, 6 h; (d) **2a–2l**, CuI, Et_3N, THF, rt, 10–15 h.

concentration, IC_{50}) against *E. coli* PDHc E1 (Table 1). The compounds had moderate inhibitory activities (IC_{50} = 6.1–75.5 μM), apart for compound **4b** (IC_{50} > 100 μM). Compounds **4h**, **4i** and **4j** proved to be potent inhibitors with IC_{50} values of 6.7, 6.9 and 6.1 μM against PDHc E1 *in vitro*, respectively. Therefore, the inhibitory rates against *Gibberella zeae in vivo* of compounds **4h**, **4i** and **4j** were further examined. By biological evaluation, compounds **4h**, **4i** and **4j** had inhibition rates of 35%, 50% and 33% at 100 μg mL^{-1} against *Gibberella zeae in vivo*, respectively.

To explore the structure–activity relationships (SAR), we first changed the R^1 group by using H (compounds **4a–4f**) or CH_3 (compounds **4g–4l**). The modifications are focused on R^1, in which the oxime ether group locates in the active site of PDHc E1. The inhibitory potencies of the two groups were obviously different (Table 1). In all categories, the inhibitory activities of the compounds in which the R^1 group is substituted with methyl (R^1 = CH_3, compounds **4g–4l**) are higher that those substituted with H (R^1 = H, compounds **4a–4f**). Subsequently, we fixed the R^1 group as methyl (R^1 = CH_3) and changed the R^2 group. The *para*-substituted analogs R^1 = CH_3, R^2 = 4-Cl (compound **4i**) showed a higher inhibitory activity (IC_{50} 6.9 ± 1.2 μM) compared to *ortho*- or *meta*-substituted compounds (R_1 = CH_3, R_2 = 2-Cl (compound **4l**) or R_1 = CH_3, R_2 = 3-Cl (compound **4g**). This implies that *para*-substitution is important for the inhibitory activity of the new oxime ether derivatives. In this case, compounds with electron-withdrawing groups on the aromatic ring (compounds **4h**, **4i**, and **4j**) were more effective that those bearing the electron-donating methoxy group (compound **4k**).

Table 1 Structures and inhibitory activities (IC_{50}) of novel thiamin diphosphate (ThDP) analog inhibitors (**4a–4l**) against *E. coli* PDHc E1 and inhibition rates (%) of **4h**, **4i** and **4j** at 100 μg mL^{-1} against *Gibberella zeae*

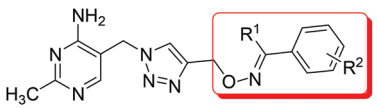

Number	Compound	R^1	R^2	IC_{50} (μM)	Inhibition rate (%)
1	**4a**	H	H	75.5 ± 0.02	N/A
2	**4b**	H	3-Cl	>100	N/A
3	**4c**	H	4-NO_2	17.8 ± 1.86	N/A
4	**4d**	H	4-Cl	59.4 ± 5.75	N/A
5	**4e**	H	4-Br	16.2 ± 1.76	N/A
6	**4f**	H	4-OCH_3	31.4 ± 1.59	N/A
7	**4g**	CH_3	3-Cl	57.8 ± 3.16	N/A
8	**4h**	CH_3	4-NO_2	6.7 ± 0.48	35
9	**4i**	CH_3	4-Cl	6.9 ± 1.19	50
10	**4j**	CH_3	4-Br	6.1 ± 0.48	33
11	**4k**	CH_3	4-OCH_3	30.2 ± 3.45	N/A
12	**4l**	CH_3	2-Cl	14.9 ± 1.25	N/A

2.3 Analyses of the interaction between the novel ThDP analog inhibitors and PDHc E1

Compound **4j** was selected for the study of the interaction mode of the novel ThDP analog inhibitors (**4a–4l**) with *E. coli* PDHc E1, because it exhibited the highest inhibitory activity (IC_{50} 6.1 ± 0.5 μM) against PDHc E1.

We performed molecular docking studies *via* site-directed mutagenesis, enzymatic assays, and fluorescence spectral analyses. As shown in Fig. 3, compound **4j** is bound to the active site of PDHc E1, which has the 'V' conformation.[14,15]

The aminopyrimidine ring of compound **4j** has similar interactions with the amino acid residues to ThDP or ThTDP in the 'V' conformation, *i.e.*, there is strong π–π stacking with the side chain ring of F602, and there are hydrogen bond interactions between the main chain oxygen of V192 and two key hydrogen atoms. These hydrogen bonds are between the N'_1 of the pyrimidine ring and the side chain of E571, and the N'_2 of the pyrimidine ring with the side chain of M194. The hydrogen bonds and the π–π stacking are responsible for the proper orientation of aminopyrimidine of the compounds to the active site of PDHc E1 (Fig. 3). The packing contacts with M194 are important in stabilizing the cofactor ThDP construction, as shown in the corresponding I415 in PDC.[29] In line with our docking prediction, the IC_{50} values of compound **4j** against the M194A mutant (69.9 μM) and V192A (57.8 μM) were about 11.5-fold and 9.5-fold higher than the value against the wild-type enzyme (6.1 μM), respectively (Fig. 4). These results also reveal that compound **4j** has stronger hydrogen bonding interactions with residues M194 (26.8-fold) and V192 (29-fold) than ThDP, based on the lower IC_{50} values for compound **4j** with M194A (69.9 μM) and V192A (57.8 μM). The

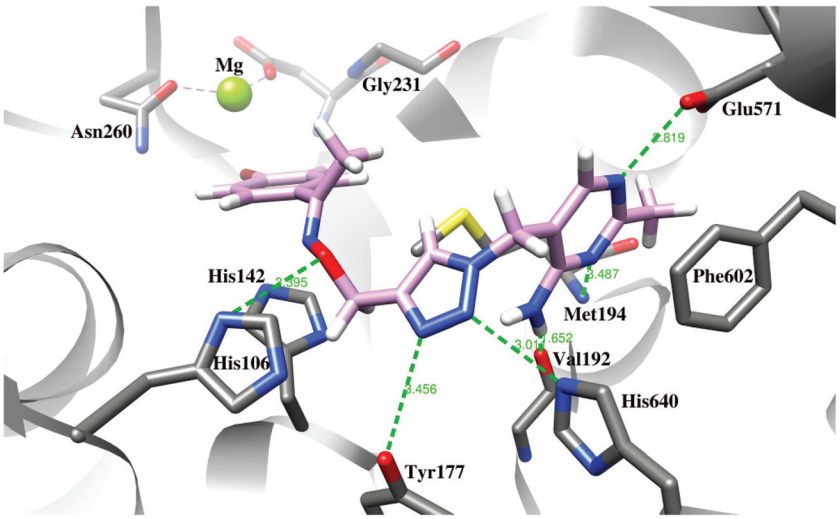

Fig. 3 Optimal binding model for compound **4j** into the active site of PDHc-E1 from *E. coli* docked by the SURFLEX module. The ligand and some key residues are presented as a stick model; hydrogen bonds are shown as dashed lines.

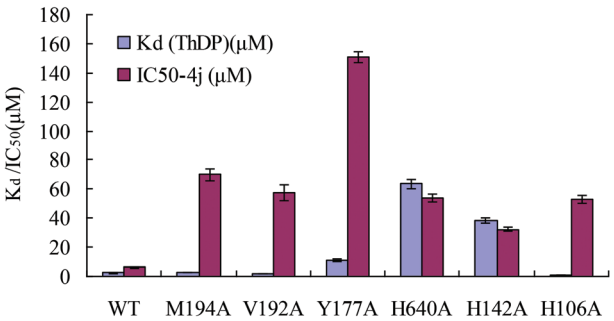

Fig. 4 The IC_{50} values of compound **4j** against the wild type (WT) and mutants of PDHc E1. The substrate is pyruvate acid, and the cofactor is ThDP.

K_d for ThDP with M194A is 2.6 μM and 2.0 μM for V192A. These results suggest that the hydrogen bonding interaction between compound **4j** and M194 or V192 is an important pharmacophoric feature.

In the middle of the 'V' conformation, the thiazolium ring of ThDP mainly interacts with residues I569 and D521.[15] During turnover, the C2 of the thiazolium ring reacts with pyruvate to form 2-α-lactyl ThDP, which in turn undergoes decarboxylation to 2-α-hydroxyethylidene-ThDP—an intermediate in the PDHc E1 reaction pathway. The Y177 residue might interact with the reaction intermediate.[12] In the vicinity of the C2 of the thiazolium ring, there is a cluster of histidine residues, including H640, H142, and H106, which likely attract and orientate the negatively charged substrate pyruvate. Residue H640 can form hydrogen bonds with pyruvate acid and is partly responsible for its proper orientation.[14,15] In compound **4j**, we substituted the thiazolium ring with the triazole ring, which forms two hydrogen bonds with residues Y177 and H640.

In our model docking study, compound **4j** exhibits a strong interaction with residues Y177 and H640. Site-directed mutagenesis and enzymatic assays showed that the IC_{50} values of compound **4j** against the Y177A (150.7 ± 3.8 μM) and H640A (53.9 ± 2.7 μM) mutants are about 39.5-fold and 8.8 higher than the value against the wild type enzyme (6.1 μM) (Fig. 4). This suggests that the hydrogen bond interaction between compound **4j** and the Y177 or H640 residue is also an important pharmacophoric feature.

Our docking results also showed that the oxime ether group attached to the aromatic ring in compound **4l** not only forms hydrogen bonds with H106, H142, and N260, but also coordinates with the metal ion (Mg^{2+}) in the active site. Site-directed mutagenesis and enzymatic assays showed that the IC_{50} values of compound **4j** against the H106 (52.7 ± 2.8 μM) and H142A (32.1 ± 1.4 μM) mutants are about 8.6 and 5.3-fold higher than the value against the wild-type enzyme (6.1 μM) (Fig. 4), suggesting that H106 and H142 play important roles in the binding of compound **4j**. However, compound **4j** has stronger interactions with H106 (66.7-fold) and similar interactions with H142 (0.8-fold) than ThDP according to the IC_{50} values for compound **4j** with H106A (52.7 ± 2.8 μM) and H142A (32.1 ± 1.4 μM) compared to the K_d for ThDP with H106A (0.8 ± 0.02 μM) and H142A (38.1 ± 1.7 μM), respectively. These results imply that H106 is one of the most important residues affecting the binding of compound **4j** to the active site of PDHc E1.

It is impossible to understand the theoretically predicted binding model directly through the enzymatic assay of the N260A mutant, because the mutant exhibits much less enzymatic activity. To further validate the interaction between compound **4j** and N260A, the binding constant (K_b) values of N260A were investigated using fluorescence spectral data. The K_b value of N260A (149 M^{-1}) is over 14-fold lower than the K_b value of the wild type enzyme (2108 M^{-1}) (Fig. 5), suggesting that there is a stronger interaction between N260 and compound **4j** than with the wild-type enzyme. These results further

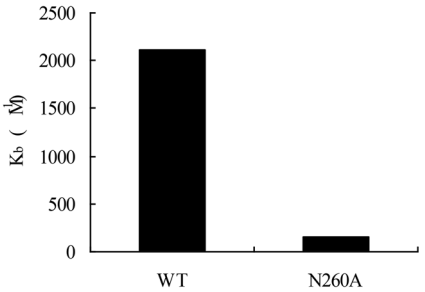

Fig. 5 Binding constants (K_b) determined by fluorescence spectral analyses for the binding of compound **4j** to the wild type (WT) and mutants of PDHc E1.

validate and explain the binding-mode between the inhibitors and the active site of PDHc E1.

3. Conclusion

In this study, we designed and synthesized a series of novel ThDP analogs as potential inhibitors of PDHc E1. Most of the compounds exhibited moderate inhibitory activities (IC_{50} = 6.1–75.5 μM). Compounds **4h**, **4i**, and **4j** were identified as potent inhibitors with IC_{50} values of 6.7, 6.9 and 6.1 μM against PDHc E1 *in vitro*, and with inhibition rates of 35%, 50% and 33% at 100 μg mL^{-1} against *Gibberella zeae in vivo*, respectively. The possible interactions of the important residues of PDHc E1 with compound **4j** were analyzed by molecular docking methods, site-directed mutagenesis, enzymatic assays, and fluorescence spectral analyses. The theoretical and experimental results are in good agreement, indicating that compound **4j** could be used as a lead compound for further optimization, and may have potential as a new microbicide.

4. Experimental procedures

4.1 General procedures

Melting points (mp) were measured on an electrothermal melting point apparatus and were uncorrected. The ^{1}H NMR spectra were recorded in DMSO-d6 on a Varian Mercury-Plus 600 spectrometer at 600 MHz. The ^{13}C NMR spectra were recorded in DMSO-d6 on a Varian Mercury-Plus 400 spectrometer at 100 MHz, and the chemical shifts were recorded in parts per million (ppm) with TMS as the internal reference. Mass spectra (MS) were obtained on a Trace MS 2000 instrument. Elemental analyses (EA) were measured on a Vario ELIII CHNSO elemental analyzer. Unless otherwise noted, reagents were purchased from commercial suppliers and used without further purification. Intermediate **3** was synthesized according to existing methods.[27]

4.1.1 General procedure for the preparation of compounds 1a–1l. A solution of benzaldehydes or acetophenones (10 mmol), hydroxylamine hydrochloride (1.39 g, 20 mmol), and anhydrous potassium carbonate (2.8 g, 20 mmol) in ethanol (10 mL) was heated under reflux until the reaction was complete, based on TLC monitoring. The solvent was then removed under reduced pressure. The residue was dissolved in water (10 mL), and the solid was filtered and recrystallized from ethanol to yield compounds **1a–1l**, which were used directly for the next step.

4.1.2 General procedure for the preparation of compounds 2a–2l. We added sodium hydroxide (0.2 g, 5 mmol) to a solution of **1a–1l** (5 mmol) and 3-bromopropyne (0.6 g, 5 mmol) in dry acetonitrile (20 mL). The mixture was heated under reflux until completion (as monitored *via* TLC), and the solvent was removed under reduced pressure. The residue was dissolved in ethyl acetate (50 mL) and washed with 0.1 M HCl, and brine and then dried and concentrated. The crude product was recrystallized with acetone to give the pure compounds **2a–2l**, which were used directly for the next step.

4.1.3 General procedure for the preparation of compounds 4a–4l. We added CuI (0.04 g, 2 mmol) to a stirred solution of 5-azidomethyl-2-methylpyrimidine-4-ylamine 3 (0.33 g, 2 mmol) and **2a–2l** (2 mmol) in THF (10 mL) followed by Et_3N (0.4 g, 4 mmol). After overnight stirring at room temperature, the reaction mixture was poured into water (50 mL), and the precipitate was collected by filtration and dried under atmospheric pressure. Recrystallization with DMF–H_2O afforded compounds **4a–4l**.

*4.1.3.1 Benzaldehyde O-((1-((4-amino-2-methylpyrimidin-5-yl) methyl)-1H-1,2,3-triazol-4-yl)methyl)oxime (**4a**).* Yellow solid; 0.59 g; Yield 92%; m.p. 170–172 °C; ^{1}H NMR (600 MHz, DMSO-d_6) δ (ppm): 2.29 (s, 3H, CH_3), 5.18 (s, 2H, CH_2), 5.44 (s, 2H, CH_2), 6.95 (s, 2H, NH_2), 7.41–7.59 (m, 5H, Ar-H), 8.02 (s, 1H, CH), 8.19 (s, 1H, CH), 8.24 (s, 1H, CH); ^{13}C NMR (100 MHz, DMSO-d_6) δ (ppm): 25.22, 46.74, 66.91, 108.45, 124.64, 126.94, 128.78, 130.03, 131.76, 143.22, 149.34, 156.16, 161.47, 167.11; MS (EI) (*m*/*z*, %): 323.4 (M^+, 5.34); Elemental Analysis for $C_{16}H_{17}N_7O$ (323.15): C, 59.43; H, 5.30; N, 30.32. Found: C, 59.65; H, 5.44; N, 30.24.

*4.1.3.2 3-Chlorobenzaldehyde O-((1-((4-amino-2-methylpyrimidin-5-yl)methyl)-1H-1,2,3-triazol-4-yl)methyl)oxime (**4b**).* Yellow solid; 0.33 g; Yield 46%; mp 154–155 °C; ^{1}H NMR (DMSO-d_6, 600 MHz): δ 2.29 (s, 3H, CH_3), 5.21 (s, 2H, CH_2), 5.44 (s, 2H, CH_2), 6.94 (s, 2H, NH), 7.44–7.50 (m, 2H, Ar-H), 7.57 (d, 1H, J = 9.0 Hz, Ar-H), 7.65 (s, 2H, CH), 7.99 (s, 1H, CH), 8.20 (s, 1H, CH), 8.26 (s, 1H, CH); ^{13}C NMR (DMSO-d_6, 100 MHz): δ 25.23, 46.83, 61.94, 100.68, 113.46, 116.36, 121.38, 124.96, 125.71, 133.81, 134.99, 135.80, 141.82, 156.38, 159.55, 161.53; MS (EI) (*m*/*z*, %): 357.2 (M^+, 2.74); Elemental Analysis for $C_{16}H_{16}ClN_7O$ (%): C, 53.71; H, 4.51; N, 27.40. Found: C, 53.51; H, 4.58; N, 27.69.

*4.1.3.3 4-Nitrobenzaldehyde O-((1-((4-amino-2-methylpyrimidin-5-yl)methyl)-1H-1,2,3-triazol-4-yl)methyl)oxime (**4c**).* Yellow solid; 0.48 g; Yield 65%; mp 214–216 °C; ^{1}H NMR (DMSO-d_6, 600 MHz): δ 2.29 (s, 3H, CH_3), 5.26 (s, 2H, CH_2), 5.43 (s, 2H, CH_2), 6.96 (s, 2H, NH), 7.86 (d, 2H, J = 9.0 Hz, Ar-H), 8.22 (s, 1H, CH), 8.27 (d, 2H, J = 8.4 Hz, CH), 8.42 (s, 1H, CH); ^{13}C NMR (DMSO-d_6, 100 MHz): δ 25.29, 46.78, 67.44, 124.02, 124.85, 127.92, 128.61, 138.05, 142.97, 147.95, 156.28, 161.43,

164.42, 167.42; MS (EI) (*m*/*z*, %): 368.1 (M^+, 2.21); Elemental Analysis for $C_{16}H_{16}N_8O_3$ (%): C, 52.17; H, 4.38; N, 30.42. Found: C, 51.72; H, 4.23; N, 30.89.

*4.1.3.4 4-Chlorobenzaldehyde O-((1-((4-amino-2-methylpyrimidin-5-yl)methyl)-1H-1,2,3-triazol-4-yl)methyl)oxime (**4d**).* Yellow solid; 0.56 g; Yield 78%; mp 185–187 °C; ^{1}H NMR (DMSO-d_6, 600 MHz): δ 2.28 (s, 3H, CH_3), 5.18 (s, 2H, CH_2), 5.43 (s, 2H, CH_2), 6.94 (s, 2H, NH), 7.48 (d, 2H, J = 8.4 Hz, Ar-H), 7.61 (d, 2H, J = 8.4 Hz, Ar-H), 7.94 (s, 2H, CH), 8.19 (s, 1H, CH), 8.25 (s, 1H, CH); ^{13}C NMR (DMSO-d_6, 100 MHz): δ 25.31, 46.97, 67.19, 125.00, 128.83, 129.16, 130.87, 134.89, 143.39, 148.63, 161.72, 162.77; MS (EI) (*m*/*z*, %): 357.3 (M^+, 3.98); Elemental Analysis for $C_{16}H_{16}ClN_7O$ (%): C, 53.71; H, 4.51; N, 27.40. Found: C, 53.32; H, 4.56; N, 27.02.

*4.1.3.5 4-Bromobenzaldehyde O-((1-((4-amino-2-methylpyrimidin-5-yl)methyl)-1H-1,2,3-triazol-4-yl)methyl)oxime (**4e**).* Yellow solid; 0.69 g; Yield 86%; mp 179–180 °C; ^{1}H NMR (DMSO-d_6, 600 MHz): δ 2.31 (s, 3H, CH_3), 3.78 (s, 3H, CH_3), 5.15 (s, 2H, CH_2), 5.47 (s, 2H, CH_2), 6.98 (s, 2H, NH), 6.98 (s, 4H, Ar-H), 7.62 (d, 2H, J = 7.8 Hz, Ar-H), 7.94 (s, 1H, CH), 8.19 (s, 1H, CH), 8.24 (s, 1H, CH); ^{13}C NMR (DMSO-d_6, 100 MHz): δ 25.29, 46.86, 67.11, 123.44, 124.81, 128.85, 131.08, 131.87, 143.25, 148.51, 156.11, 161.52, 162.44; MS (EI) (*m*/*z*, %): 403.3 (M^+ + 2, 2.57), 401.2 (M^+, 1.94); Elemental Analysis for $C_{16}H_{16}BrN_7O$ (%): C, 47.44; H, 4.01; N, 24.37. Found: C, 46.95; H, 4.10; N, 24.21.

*4.1.3.6 4-Methoxybenzaldehyde O-((1-((4-amino-2-methylpyrimidin-5-yl)methyl)-1H-1,2,3-triazol-4-yl)methyl)oxime (**4f**).* Yellow solid; 0.21 g; Yield 30%, mp 100–101 °C; ^{1}H NMR (DMSO-d_6, 600 MHz): δ 2.31 (s, 3H, CH_3), 3.78 (s, 3H, OCH_3), 5.15 (s, 2H, CH_2), 5.47 (s, 2H, CH_2), 6.98 (s, 4H, Ar + NH), 7.54 (s, 2H, Ar-H), 8.17 (s, 2H, CH); ^{13}C NMR (DMSO-d_6, 100 MHz): δ 25.31, 36.09, 46.96, 67.19, 108.62, 125.00, 128.84, 129.16, 130.87, 134.89, 143.39, 148.63, 156.33, 161.72, 162.77; MS (EI) (*m*/*z*, %): 354.4 (M^+ + 1, 1.37), 353.3 (M^+, 6.40); Elemental Analysis for $C_{17}H_{19}N_7O_2$ (%): C, 57.78; H, 5.42; N, 27.75. Found: C, 57.30; H, 5.41; N, 27.56.

*4.1.3.7 1-(3-Chlorophenyl)ethanone O-((1-((4-amino-2-methylpyrimidin-5-yl)methyl)-1H-1,2,3-triazol-4-yl)methyl)oxime (**4g**).* Yellow solid; 0.47 g; Yield 64%; mp 131–133 °C; ^{1}H NMR (DMSO-d_6, 600 MHz): δ 2.15 (s, 3H, CH_3), 2.29 (s, 3H, CH_3), 5.22 (s, 2H, CH_2), 5.44 (s, 2H, CH_2), 6.95 (s, 2H, NH), 7.42–7.48 (m, 2H, Ar-H), 7.60 (d, 1H, J = 7.2 Hz, Ar-H), 7.67 (s, 1H, Ar-H), 8.00 (s, 1H, CH), 8.19 (s, 1H, CH); ^{13}C NMR (DMSO-d_6, 100 MHz): δ 12.43, 25.25, 46.74, 67.08, 108.38, 108.30, 124.63, 125.59, 129.10, 130.32, 133.34, 137.91, 143.34, 153.69, 156.31, 161.49, 167.04; MS (EI) (*m*/*z*, %): 373.3 (M^+ + 2, 1.96), 371.3 (M^+, 8.28); Elemental Analysis for $C_{17}H_{18}ClN_7O$ (%): C, 54.91; H, 4.88; N, 26.37. Found: C, 54.48; H, 4.62; N, 26.26.

*4.1.3.8 1-(4-Nitrophenyl)ethanone O-((1-((4-amino-2-methylpyrimidin-5-yl)methyl)-1H-1,2,3-triazol-4-yl)methyl)oxime (**4h**).* Yellow solid; 0.46 g; yield 60%; mp 222–224 °C; ^{1}H NMR (DMSO-d_6, 600 MHz): δ 2.21 (s, 3H, CH_3), 2.30 (s, 3H, CH_3), 5.27 (s, 2H, CH_2), 5.47 (s, 2H, CH_2), 6.98 (s, 2H, NH), 7.89 (s, 2H, Ar-H), 8.21 (s, 1H, CH), 8.25 (d, 2H, J = 7.2 Hz, Ar-H); ^{13}C NMR (DMSO-d_6, 100 MHz): δ 11.87, 24.83, 46.27, 66.81, 108.68, 123.11, 124.31, 126.56, 141.35, 142.76, 147.15, 152.98, 155.63, 160.98, 167.12; MS (EI) (*m*/*z*, %): 383.3 (M^+ + 1, 1.28), 382.3 (M^+, 8.05); Elemental Analysis for $C_{17}H_{18}N_8O_3$ (%): C, 53.40; H, 4.74; N, 29.30. Found: C, 53.61; H, 4.31; N, 29.12.

*4.1.3.9 1-(4-Chlorophenyl)ethanone O-((1-((4-amino-2-methylpyrimidin-5-yl)methyl)-1H-1,2,3-triazol-4-yl)methyl)oxime (**4i**).* Yellow solid; 0.67 g; yield 90%; mp 184–186 °C; ^{1}H NMR (DMSO-d_6, 600 MHz): δ 2.14 (s, 3H, CH_3), 2.29 (s, 3H, CH_3), 5.20 (s, 2H, CH_2), 5.44 (s, 2H, CH_2), 6.98 (s, 2H, NH), 7.47 (s, 2H, Ar-H), 7.64 (s, 2H, Ar-H), 8.19 (s, 1H, CH); ^{13}C NMR (DMSO-d_6, 100 MHz): δ 12.25, 25.50, 46.74, 66.91, 122.69, 124.68, 127.85, 130.06, 131.31, 134.88, 143.51, 153.80, 155.72, 161.31, 168.79; MS (EI) (*m*/*z*, %): 373.2 (M^+ + 2, 2.06), 371.3 (M^+, 7.27); Elemental Analysis for $C_{17}H_{18}ClN_7O$ (%): C, 54.91; H, 4.88; N, 26.37. Found: C, 54.45; H, 4.75; N, 26.18.

*4.1.3.10 1-(4-Bromophenyl)ethanone O-((1-((4-amino-2-methylpyrimidin-5-yl)methyl)-1H-1,2,3-triazol-4-yl)methyl)oxime (**4j**).* Yellow solid; 0.56 g; Yield 66%; mp 180–183 °C; ^{1}H NMR (DMSO-d_6, 600 MHz): δ 2.13 (s, 3H, CH_3), 2.30 (s, 3H, CH_3), 5.20 (s, 2H, CH_2), 5.49 (s, 2H, CH_2), 7.02 (s, 2H, NH), 7.57 (d, 2H, J = 7.2 Hz, Ar-H), 7.60 (d, 2H, J = 7.8 Hz, Ar-H), 8.19 (s, 1H, CH); ^{13}C NMR (DMSO-d_6, 100 MHz): δ 12.25, 25.50, 46.74, 66.91, 122.69, 124.68, 127.85, 130.06, 131.31, 134.88, 143.51, 153.80, 155.72, 161.31, 168.79; MS (EI) (*m*/*z*, %): 417.2 (M^+ + 2, 5.79), 415.2 (M^+, 6.78); Elemental Analysis for $C_{17}H_{18}BrN_7O$ (%): C, 49.05; H, 4.36; N, 23.55. Found: C, 49.23; H, 4.54; N, 23.91.

*4.1.3.11 1-(4-Methoxyphenyl)ethanone O-((1-((4-amino-2-methylpyrimidin-5-yl)methyl)-1H-1,2,3-triazol-4-yl)methyl)oxime (**4k**).* Yellow solid; 0.47 g; Yield 64%; mp 154–156 °C; ^{1}H NMR (DMSO-d_6, 600 MHz): δ 2.12 (s, 3H, CH_3), 2.29 (s, 3H, CH_3), 3.77 (s, 3H, OCH_3), 5.16 (s, 2H, CH_2), 5.43 (s, 2H, CH_2), 6.95 (d, 4H, J = 9.0 Hz, Ar-H + NH), 7.58 (d, 2H, J = 9.0 Hz, Ar-H), 8.01 (s, 1H, CH), 8.17 (s, 1H, CH); ^{13}C NMR (DMSO-d_6, 100 MHz): δ 12.43, 25.22, 46.69, 55.19, 66.71, 108.40, 113.81, 124.54, 127.37, 128.22, 143.64, 154.21, 156.28, 160.17, 161.51, 167.09; MS (EI) (*m*/*z*, %): 367.4 (M^+, 10.04); Elemental Analysis for $C_{18}H_{21}N_7O$ (%): C, 58.84; H, 5.76; N, 26.69. Found: C, 58.58; H, 5.62; N, 26.13.

*4.1.3.12 1-(2-Chlorophenyl)ethanone O-((1-((4-amino-2-methylpyrimidin-5-yl)methyl)-1H-1,2,3-triazol-4-yl)methyl)oxime (**4l**).* Yellow solid, 0.49 g; Yield 67%; mp 180–182 °C; ^{1}H NMR (DMSO-d_6, 600 MHz): δ 2.14 (s, 3H, CH_3), 2.29 (s, 3H, CH_3), 5.20 (s, 2H, CH_2), 5.45 (s, 2H, CH_2), 6.98 (s, 2H, NH), 7.46 (s, 2H, Ar-H), 7.64 (s, 2H, Ar-H), 8.19 (s, 1H, CH); ^{13}C NMR (DMSO-d_6, 100 MHz): δ 12.35, 25.22, 46.73, 66.94, 109.30, 124.63, 127.67, 128.46, 134.01, 134.60, 143.46, 153.76, 155.94, 158.09, 161.45, 167.35; MS (EI) (*m*/*z*, %): 373.3 (M^+ + 2, 2.78), 371.3 (M^+, 7.22); Elemental Analysis for $C_{17}H_{18}ClN_7O$ (%): C, 54.91; H, 4.88; N, 26.37. Found: C, 54.18; H, 4.72; N, 26.46.

4.2 Structure-based docking

The crystallographic coordinates of PDHc-E1 with ThDP from *E. coli* (PDB code: 1L8A) were obtained from the Brookhaven Data Bank for structure-based docking rational analyses. Hydrogen atoms were added to the structure to allow for

appropriate ionization at physiological pH. The protonated state of several important residues such as His106, His142, Tyr177, Met194, Glu571, and His640 were adjusted with SYBYL7.3 (Tripos, St. Louis, MO, USA) to form hydrogen bonds with the ligand. Molecular docking analysis was performed with the SURFLEX module of the SYBYL package to explore the interaction model for the active site of PDHc-E1 with its ligand, especially with cofactor ThDP. All atoms located within 6.5 Å from any atom of the cofactor ThDP were selected into the active site, and the corresponding amino acid residue was thus involved with the active site only if one of its atoms were selected. Other default parameters were adopted in the SURFLEX-docking calculations. All calculations were performed on the CCNU Grid website http://www.202.114.32.71:8090/ccnu/chem/platform.xml.

4.3 Inhibitory enzymatic activity evaluation and site-directed mutagenesis of PDHc E1

To evaluate the inhibitory activity of the compounds against PDHc E1, the half maximal inhibitory concentration (IC_{50}) values of the compounds were determined at the PDHc E1 enzyme level *in vitro*. The cloning, expression, purification and activity of PDHc E1 were carried out as described previously.[18] ThDP and pyruvate were purchased from Sigma. Enzyme activities were measured as described previously.[18] For IC_{50} determination, we used a standard reaction mixture containing 50 mM K_3PO_4 (pH 6.4), 0.4 mM 2, 6-dichlorophenolindophenol (DCIP), 50 μM sodium pyruvate as the substrate, 5 μg PDHc E1 purified enzyme and 50 μM ThDP. The compounds from 0 to 200 μM were incubated for 5 min with PDHc E1 at 37 °C before the substrate (pyruvate) was added. The IC_{50} values were determined by nonlinear least-squares fitting of the data using the Hill kinetic equations in the Growth/sigmoidal model from origin 7.0 software as described previously.[30]

Site-directed mutagenesis of PDHc E1 was accomplished by the introduction of specific base changes into a double-stranded DNA plasmid, as described previously.[30] DNA encoding of the wild-type PDHc E1 cloned into the pMAL-C_{2x}-PDHc-E1 was used as a template for mutagenesis. The standard PCR mixture contained 50–100 ng of template DNA and 100–200 ng of each mutagenizing primer. The methylated plasmid was digested with DpnI, and 4 μL of each reaction was used to transform the DH5α competent cells. All mutations were confirmed by DNA sequencing. Verified plasmids containing the desired mutations were transformed into the *E. coli* TB1 strain. The mutant PDHc E1 proteins were purified in the same manner as the wild-type PDHc E1.

4.4 Inhibitory activity evaluation of compounds against *Gibberella zeae in vivo*

Inhibitory activity evaluation of compounds **4h**, **4i**, and **4j** against *Gibberella zeae in vivo* were tested and their relative inhibitory ratio (%) had been determined using the mycelium growth rate method.[31] The compound was dissolved in acetone. The solution was diluted in water to the required concentration. The mycelial elongation (mm) of *Gibberella zeae* settlements was measured after 48 h of culture on potato glucose solid medium. The final concentration of the compound in medium was 100 μg mL^{-1}. Three replicates of each test were carried out. The growth inhibition rates (I) were calculated using the equation: $I = [(C - T)/C] \times 100\%$, where C is the average diameter of mycelia in the presence of these compounds. The inhibition ratio of these compounds, at the dose of 100 μg mL^{-1}, are shown in Table 1.

4.5 Fluorescence spectral analyses

Fluorescence spectral analyses were carried out as described previously.[32] All fluorescent measurements were carried out on a FluoreMax-P fluorescence spectrophotometer (HORIBA JOBIN YVON, France) equipped with a xenon lamp source and 1.0 cm quartz cell. The emission spectrum was recorded in the 305–500 nm range with excitation at 290 nm. The fluorescence quenching experiments of PDHc E1 or its mutants (2 μM) were performed at different concentrations of compounds by applying a 1 cm path length cuvette. The appropriate blank measurement corresponding to the buffer was subtracted to correct the background fluorescence. The binding constant (K) was calculated according to the equation: $\ln\frac{F_0-F}{F} = \ln K + n\ln[Q]$, where F_0 and F are the fluorescence intensities without and with the ligand, respectively. Term [Q] denotes the concentration of the quencher. A plot of $\ln[(F_0 - F)/F]$ *vs.* $\ln[Q]$ gave a straight line using least squares analysis. The Y-intercept was equal to $\ln K$ (where K is equal to the binding constant).

Acknowledgements

This work was supported by the National Basic Research Program of China (no. 2010CB126100), the Natural Science Foundation of China (no. 21472061, 21373094, 21272089, 21172089, 21172090, 21072073, 20873049, 20872044, 30900054, and 30800169), the Program for New Century Excellent Talents in University (no. NCET-06-0673), the Program for Changjiang Scholars and Innovative Research Team in University (PCSIRT no. IRT0953), the Program for Academic Leader in Wuhan Municipality (no. 201150530150), the Special Fund for Basic Scientific Research of Central Colleges of Ministry of Education (no. CCNU09A01010, CCNU10C01002, and CCNU10A02006), and the Research Fund for the Doctoral Program of Higher Education of China (200805581146).

References

1 D. Fernández-Ortuño, F. Chen and G. Schnabel, *Plant Dis.*, 2012, **96**, 1198.
2 F. Qadri, A. M. Svennerholm, A. S. G. Faruque and R. B. Sack, *Clin. Microbiol. Rev.*, 2005, **18**, 465.
3 H. Y. Sun, H. C. Wang, Y. Chen, H. X. Li, C. J. Chen and M. G. Zhou, *Plant Dis.*, 2010, **94**, 551.

4 A. S. Puertoa, J. G. Fernandeza, J. D. L. Castillob, M. J. S. Pinoa and G. P. Anguloa, *Diagn. Microbiol. Infect. Dis.*, 2006, **54**, 135.
5 F. Jordan, N. Nemeria, F. Guo, I. Baburina, Y. Gao, A. Kahyaoglu, H. Li, J. Wang, J. Yi, J. R. Guest and W. Furey, *Biochim. Biophys. Acta, Protein Struct. Mol. Enzymol.*, 1998, **1385**, 287.
6 W. Wei, H. Li, N. Nemeria and F. Jordan, *Protein Expression Purif.*, 2003, **28**, 140.
7 R. H. Jackson and T. P. Singer, *J. Biol. Chem.*, 1983, **258**, 1857.
8 A. Brown, N. Nemeria, J. Yi, D. Zhang, W. B. Jordan, R. S. Machado, J. R. Guest and F. Jordan, *Biochemistry*, 1997, **36**, 8071.
9 E. Schoenbrunn-Hanebeck, B. Laber and N. Amrhein, *Biochemistry*, 1990, **29**, 4880.
10 M. A. Apfel, B. H. Ikeda, D. C. Speckhard and P. A. Frey, *J. Biol. Chem.*, 1984, **259**, 2905.
11 J. A. Gutowski and G. E. Lienhard, *J. Biol. Chem.*, 1976, **251**, 2863.
12 N. Nemeria, Y. Yan, Z. Zhang, A. M. Brown, P. Arjunan, W. Furey, J. R. Guest and F. Jordan, *J. Biol. Chem.*, 2001, **276**, 45969.
13 K. Agyei-Owusu and F. J. Leeper, *FEBS J.*, 2009, **276**, 2905.
14 P. Arjunan, N. Nemeria, A. Brunskill, K. Chandrasekhar, M. Sax, Y. Yan, F. Jordan, J. R. Guest and W. Furey, *Biochemistry*, 2002, **41**, 5213.
15 P. Arjunan, K. Chandrasekhar, M. Sax, A. Brunskill, N. Nemeria, J. F. Frank and W. Furey, *Biochemistry*, 2004, **43**, 2405.
16 H. W. He, J. L. Yuan, H. Peng, T. Chen, P. Shen, S. Q. Wan, Y. J. Li, H. L. Tan, Y. H. He, J. B. He and Y. Li, *J. Agric. Food Chem.*, 2011, **59**, 4801.
17 H. W. He, H. Peng, T. Wang, C. B. Wang, J. L. Yuan, T. Chen, J. B. He and X. S. Tan, *J. Agric. Food Chem.*, 2013, **61**, 2479.
18 Y. L. Ren, J. B. He, L. L. Feng, X. Liao, J. Jin, Y. J. Li, Y. Cao, J. Wan and H. W. He, *Bioorg. Med. Chem.*, 2011, **19**, 7501.
19 K. Pericherla, P. Khedar, B. M. Khungar and A. Kumar, *Tetrahedron Lett.*, 2012, **53**, 6761.
20 K. Slamova, P. Marhol, K. Bezouska, L. Lindkvist, S. Hansen, V. Kren and H. H. Jensen, *Bioorg. Med. Chem. Lett.*, 2010, **20**, 4263.
21 S. Emami, M. Falahati, A. Banifatemi and A. Shafiee, *Bioorg. Med. Chem.*, 2004, **12**, 5881.
22 A. Rossello, S. Bertini, A. Lapucci, M. Macchia, A. Martinelli, S. Rapposelli, E. Herreros and B. Macchia, *J. Med. Chem.*, 2002, **45**, 4903.
23 H. J. Park, K. Lee, S. J. Park, B. Ahn, J. C. Lee, H. Y. Cho and K. I. Lee, *Bioorg. Med. Chem. Lett.*, 2005, **15**, 3307.
24 C. Ramalingan, Y. T. Park and S. Kabilan, *Eur. J. Med. Chem.*, 2006, **41**, 683.
25 J. T. Li, Y. X. Chen, X. L. Li and H. J. Deng, *Asian J. Chem.*, 2007, **19**, 2236.
26 M. M. Pakulski, S. K. Mahato, M. J. Bosiak, M. P. Krzeminski and M. Zaidlewicz, *Tetrahedron: Asymmetry*, 2012, **23**, 716.
27 K. M. Erixon, C. L. Dabalos and F. J. Leeper, *Org. Biomol. Chem.*, 2008, **6**, 3561.
28 M. Meldal and C. W. Tornøe, *Chem. Rev.*, 2008, **108**, 2592.
29 F. Jordan, Z. Zhang and E. Sergienko, *Bioorg. Chem.*, 2002, **30**, 188.
30 L. L. Feng, Y. Sun, H. Deng, D. Li, J. Wan, X. F. Wang, W. W. Wang, X. Liao, Y. L. Ren and X. P. Hu, *FEBS J.*, 2014, **281**, 916.
31 N. C. Chen, *Bioassay of pesticides*, Beijing Agricultural University Press, Beijing, China, 1991, pp. 161–162.
32 Y. Sun, X. Liao, D. Li, L. L. Feng, J. Li, X. F. Wang, J. Jin, F. Yi, L. Zhou and J. Wan, *Spectrochim. Acta, Part A*, 2012, **89**, 337.

